Sliding-mode Velocity and Yaw Control of a 4WD Skid-steering Mobile Robot

Eric Lucet, Christophe Grand and Philippe Bidaud

Eric Lucet
Robosoft, Technopole d'Izarbel, F-64210 Bidart, France. e-mail: eric.lucet@robosoft.fr

Christophe Grand and Philippe Bidaud
ISIR-UPMC, UMR 7222, F-75005 Paris, France. e-mail: christophe.grand@upmc.fr

Abstract The subject of this paper is the design and implementation of a robust dynamic feedback controller, based on the dynamic model of the four-wheel skid-steering RobuFAST A robot, undergoing high-speed turns. The control inputs are respectively the linear velocity and the yaw angle. The main objective of this paper is to formulate a sliding mode controller, robust enough to obviate the knowledge of the forces within the wheel-soil interaction, in the presence of sliding phenomena and ground-level fluctuations. Finally, experiments are conduced on a slippery ground to ascertain the efficiency of the control law.

1 Introduction

This paper considers the problem of a robust control of high-speed wheeled robots maneuvering on slippery grounds with varying properties.

The dynamic control of skid-steering robots was studied in particular in [1] using a dynamic feedback linearization paradigm for a model-based controller which minimizes lateral skidding by imposing the longitudinal position of the instantaneous center of rotation. Another algorithm reported in [2], offers a good robustness considering uncertainties on the robot dynamic parameters. In addition to the nonholonomic constraint of the controller designed by Caracciolo, the authors use an oscillator signal [3] for kinematic control.

We suggest a strategy based on the sliding-mode theory. The sliding-mode control law—or, more precisely, controller with variable structure generating a sliding regime—aims to obtain, by feedback, a dynamics widely independent from that of the process and its possible variations. Hence, the controller can be considered as belonging to the class of robust controllers. The sliding-mode control appears attractive for the handling of nonlinear and linear systems, multivariable and single-variable systems, as well as model or trajectory pursuit problems and problems of regulation.

Sliding-mode control allows a decoupling design procedure and good disturbance rejection. This control scheme is robust to the uncertainties in the dynamic parameters of the system, and is easily implementable. Indeed, robust control is widely used in the literature; particular [4] and [5] propose examples of dynamic sliding-mode controllers without taking into account the vehicle dynamics. In [6], and then [7], the authors consider the dynamics model of a unicycle system during the implementation of their control law by using the kinematic nonholonomic non-skidding constraint. The non compliance with nonholonomic constraints in real conditions is taken into account in [8]. However, the problem is formalized for the particular case of the partially linearized dynamics model of a unicycle robot.

Using the sliding-mode theory, we suggest here a new approach to control a fast skid-steering mobile robot with wheel torques as inputs, based on its dynamics model. The objective is to force the mobile robot to follow a desired path at rel-

atively high speed, by controlling its yaw angle and its longitudinal velocity. The ground considered is nominally horizontal and relatively smooth as compared with the wheel dimensions. If most of the control laws consider that the conditions of movement without slippage are satisfied, this hypothesis is not valid at high speed, where wheel slippage becomes significant, thus reducing the robot stability. The implemented controller will have to be robust with respect to these phenomena in order to ensure an efficient path-following.

2 Application to a Skid-steering Mobile Robot

Because it has proved to be robust enough to obviate the modeling of the forces in the wheel-soil interaction in the presence of slippage, a sliding-mode controller is applied to a skid-steering mobile robot. This scheme ensures the control of the hending velocity and the yaw angle.

2.1 System Modeling

Considering the integer $i \in [1;N]$ with N denoting the number of wheels of the skid-steering robot, let us define the two generalized torques τ_u and τ_θ, uniformly distributed throughout the torques τ_i of each wheel i according to the equations:

$$\tau_u = \sum_{i=1}^{N} \tau_i; \quad \tau_\theta = \sum_{i=1}^{N} \frac{-w_i}{R} \tau_i \tag{1}$$

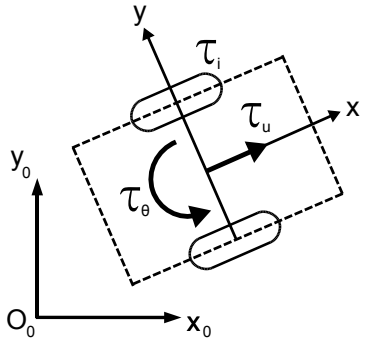

Fig. 1 Torques dispatching

2.2 Control of the Yaw Angle

2.2.1 Design of the Control Law

In the case of a skid-steering robot, let us express the yaw movement dynamics from the equations of the general dynamics:

$$I_z \dot{r} = \sum_{i=1}^{N} (-w_i F_{xi} + l_i F_{yi}) \tag{2}$$

Applying Newton's second law to the ith wheel, we have:

$$I_\omega \dot{\omega}_i = \tau_i - R F_{xi} \tag{3}$$

with R the wheel radius and I_w its centroidal moment of inertia, assumed to be the same for all the wheels.

Considering the torque definition τ_θ and equations (3) and (2), we have :

$$\dot{r} = \lambda \tau_\theta + \lambda_\theta \dot{\omega} + \mathbf{D}_\theta \mathbf{F_y} \tag{4}$$

with:

$$\lambda = \frac{1}{I_z}; \lambda_\theta = \frac{I_\omega}{I_z R} [\cdots w_i \cdots]; \dot{\omega} = [\cdots \dot{\omega}_i \cdots]^T; \mathbf{D}_\theta = \frac{1}{I_z} [\cdots l_i \cdots]; \mathbf{F}_y = [\cdots F_{yi} \cdots]^T$$

The correction of the vehicle steering does not permit the system to converge to the desired trajectory. It is also necessary to correct the lateral error; otherwise, the system will aim towards a movement parallel to the reference path, not necessarily reaching it. This is why we are going to modify the desired yaw angle, as proposed in other works [9].

The robot has to follow the path, the reference point P being all the time the projection of its centre of mass G on this one. To take into account the lateral error, we add to θ_d a term limited between $-\frac{\pi}{2}$ and $\frac{\pi}{2}$ excluded, increasing with the lateral error d, the function defining this term being also odd to permit a similar behavior on both sides of the path. We thus define the modified desired steering angle $\tilde{\theta}_d$ such as:

$$\tilde{\theta}_d = \theta_d + \arctan\left(\frac{d}{d_0}\right) \tag{5}$$

with d_0 a positive gain of regulation of the intensity of the correction of the lateral distance d.

For the implementation of the controller, we proceed to a temporary change of the control variable by replacing the generalized torque τ_θ. To this end, we introduce $c_{d\theta}$, which represents the control law to be applied and $n(\theta, r, \dot{r})$ the uncertainty function on θ, r and $\dot{r}$ in the dynamics equations. We thus have the relation:

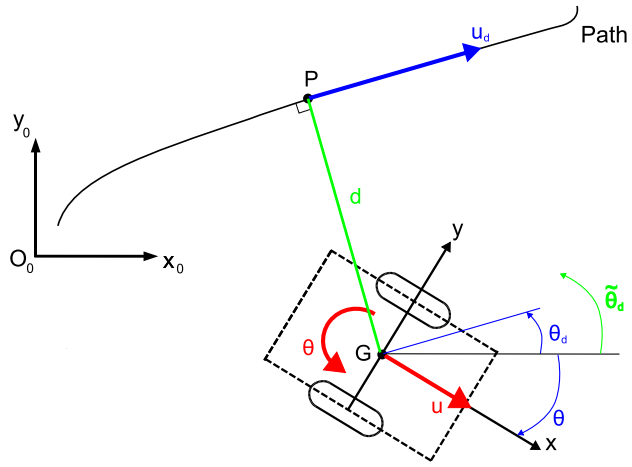

Fig. 2 Path following parameters

$$\dot{r} = c_{d\theta} - n(\theta, r, \dot{r}) \tag{6}$$

The control law is chosen as:

$$c_{d\theta} = \ddot{\tilde{r}}_d + K_p^\theta \varepsilon_\theta + K_d^\theta \dot{\varepsilon}_\theta + \sigma_\theta \tag{7}$$

which includes four terms:

- $\ddot{\tilde{r}}_d$, the second derivative of $\tilde{\theta}_d$, an anticipative term;
- $\varepsilon_\theta = \tilde{\theta}_d - \theta$, the yaw-angle error;
- K_p^θ and K_d^θ, two positive constants that permit to define the settling time and the overshoot of the closed-loop system;
- σ_θ, the sliding-mode control law.

2.2.2 Error State Equation

The second derivative of ε_θ is given below:

$$\begin{aligned} \ddot{\varepsilon}_\theta &= \ddot{\tilde{r}}_d - \dot{r} = \ddot{\tilde{r}}_d - c_{d\theta} + n \\ &= \ddot{\tilde{r}}_d - \left(\ddot{\tilde{r}}_d + K_p^\theta \varepsilon_\theta + K_d^\theta \dot{\varepsilon}_\theta + \sigma_\theta\right) + n \\ &= -K_p^\theta \varepsilon_\theta - K_d^\theta \dot{\varepsilon}_\theta + (n - \sigma_\theta) \end{aligned} \tag{8}$$

Let the error state vector be: $\mathbf{x} = \left[\varepsilon_\theta, \dot{\varepsilon}_\theta\right]^T$, the state equation then becoming

$$\dot{\mathbf{x}} = \mathbf{A}\mathbf{x} + \mathbf{B}(\mathbf{n} - \sigma_\theta) \tag{9}$$

with :

$$\mathbf{A} = \begin{pmatrix} 0 & 1 \\ -K_p^\theta & -K_d^\theta \end{pmatrix} \; ; \; \mathbf{B} = \begin{pmatrix} 0 \\ 1 \end{pmatrix}$$

If $\sigma_\theta = 0$ (and so $n = 0$, without model error to correct), the system is linear, and we choose the values of K_p^θ and K_d^θ as $K_p^\theta = \omega_n^2$ and $K_d^\theta = 2\zeta\omega_n$ in order to define a second-order system. ω_n is the pulsation and ζ the damping ratio. To define numerical values, the 5% settling time T_r is introduced: $T_r = \frac{4.2}{\zeta\omega_n}$.

2.2.3 Stability Analysis

To approach the problem of the stability of the closed-loop system, the pursuit of the desired yaw angle $\tilde{\theta}_d$ can be studied by using the candidate Lyapunov function $V = \mathbf{x}^T\mathbf{P}\mathbf{x}$, with $\mathbf{P}$ a positive definite symmetric matrix. According to the Lyapunov theorem, [10], the state $\mathbf{x} = \mathbf{0}$ is stable if and only if:

$$V(0) = 0 \; ; \; \forall \mathbf{x} \neq \mathbf{0} \;\; \mathbf{V}(\mathbf{x}) > \mathbf{0} \textbf{ and } \dot{\mathbf{V}}(\mathbf{x}) < \mathbf{0} \tag{10}$$

The first two foregoing relations being verified at once, it remains to establish the third. From eq.(9), we compute the derivative:

$$\begin{aligned} \dot{V}(\mathbf{x}) &= \dot{\mathbf{x}}^T\mathbf{P}\mathbf{x} + \mathbf{x}^T\mathbf{P}\dot{\mathbf{x}} \\ &= \left(\mathbf{x}^T\mathbf{A}^T + n\mathbf{B}^T - \sigma_\theta\mathbf{B}^T\right)\mathbf{P}\mathbf{x} + \mathbf{x}^T\mathbf{P}\left(\mathbf{A}\mathbf{x} + \mathbf{B}n - \mathbf{B}\sigma_\theta\right) \\ &= \mathbf{x}^T\left(\mathbf{A}^T\mathbf{P} + \mathbf{P}\mathbf{A}\right)\mathbf{x} + 2\mathbf{x}^T\mathbf{P}\mathbf{B}\left(n - \sigma_\theta\right) \end{aligned} \tag{11}$$

The last equality is obtained by considering that $s = \mathbf{B}^T\mathbf{P}\mathbf{x}$ is a scalar, so $\mathbf{B}^T\mathbf{P}\mathbf{x} = \mathbf{x}^T\mathbf{P}\mathbf{B}$. Then, the matrix $\mathbf{P}$ is computed to obtain the equation (12) below:

$$\mathbf{A}^T\mathbf{P} + \mathbf{P}\mathbf{A} = -\mathbf{Q}_l \tag{12}$$

with $\mathbf{Q}_l$ a positive defined symmetric matrix; it is the Lyapunov equation. In that case, the equation (11) is reformulated:

$$\dot{V} = -\mathbf{x}^T\mathbf{Q}_l\mathbf{x} + 2\mathbf{x}^T\mathbf{P}\mathbf{B}\left(n - \sigma_\theta\right)$$

It is necessary that $\dot{V}$ be negative for stability. The first term of the right-hand side of the above equation is negative, while the second term vanishes if $\mathbf{x}$ lies in the kernel of $\mathbf{B}^T\mathbf{P}$. Outside the kernel, the second term has to be as small as possible. Let us define $s = \mathbf{B}^T\mathbf{P}\mathbf{x}$. The equality $s = 0$ is the ideal case, represents the hyperplane defining the sliding surface. Keeping the sliding surface s equal to zero is then equivalent to the pursuit of the vector of the desired states, the error state vector $\mathbf{x}$ being zero. As this surface reaches the origin, the static error ε_θ will be equal to zero.

We suggest the sliding-mode control law σ_θ:

$$\sigma_\theta = \mu \frac{s}{|s|} \tag{13}$$

where we use the norm of s, and μ is a positive scalar. This choice leads to:

$$s(n-\sigma_\theta) = sn - \mu \frac{s^2}{|s|} = sn - \mu |s| \leq |s|(|n| - \mu)$$

Thus, the conditions of convergence are: $|n| \leq n_{Max} < \infty$ and a choice of $\mu > n_{Max}$ which guarantee the Lyapunov theorem hypotheses. Stability is guaranteed if we adopt the control law (13).

Finally, we have the control law:

$$c_{d\theta} = \dot{\tilde{r}}_d + K_p^\theta \varepsilon_\theta + K_d^\theta \dot{\varepsilon}_\theta + \mu \frac{s}{|s|} \tag{14}$$

with $s = \mathbf{B}^T \mathbf{P} \mathbf{x}$.

2.2.4 Solution the Lyapunov Equation

To solve the equation (12), the matrix $\mathbf{Q}_l$ is chosen as:

$$\mathbf{Q}_l = \begin{pmatrix} a & 0 \\ 0 & b \end{pmatrix}$$

with $a > 0$ and $b > 0$. With matrix $\mathbf{A}$ determined, matrix $\mathbf{P}$ is:

$$\mathbf{P} = \begin{pmatrix} \frac{1.05b}{\zeta^2 T_r} + \frac{5a\zeta^2 T_r}{21} + \frac{aT_r}{16.8} & \frac{a\zeta^2 {T_r}^2}{35.28} \\ \frac{a\zeta^2 {T_r}^2}{35.28} & \frac{bT_r}{16.8} + \frac{a\zeta^2 T_r^3}{296.352} \end{pmatrix} \tag{15}$$

We determine the influence of the $\mathbf{Q}_l$ matrix components. As previously defined, the equation of the sliding hyperplane is:

$$s = \mathbf{B}^T \mathbf{P} \mathbf{x} = p_{21} \varepsilon_\theta + p_{22} \dot{\varepsilon}_\theta$$

with p_{21} and p_{22} being two entries of the positive-definite and symmetric matrix $\mathbf{P}$ occurring in the expression of the candidate Lyapunov function. Here, this hyperplane is a straight line.

At the neighborhood of this straight line, we have: $s = p_{21} \varepsilon_\theta + p_{22} \dot{\varepsilon}_\theta = 0$, whose integral is:

$$\varepsilon_\theta(t) = \varepsilon_\theta(\tau) \exp\left[\left(-p_{21}/p_{22}\right)(t-\tau)\right]$$

with $\varepsilon_\theta(\tau)$ a real constant which depends on the initial conditions at $t = \tau$, when the system arrives at the neighborhood of the sliding straight line.

Consequently, we derive from this solution that to correct the error, it is necessary to increase the value of p_{21} and to decrease the value of p_{22}. According to expression (15) for $\mathbf{P}$, we know these two parameters. Hence, to eliminate quickly the position error, it is necessary to increase the value of a and to decrease that of b. As far as the sliding straight line is concerned, this modification of the various coefficients increases the straight line slope.

2.3 Control of the Longitudinal Velocity

We use the dynamics model according to the longitudinal axis from the equations of the general dynamics:

$$M(\dot{u} - rv) = \sum_{i=1}^{N} F_{xi} \tag{16}$$

From the definition of the torque τ_u and equations (3) and (16), we solve for the longitudinal acceleration:

$$\dot{u} = \gamma\tau_u + \Lambda_u \sum_{i=1}^{N} \dot{\omega}_i + rv \tag{17}$$

with:

$$\gamma = \frac{1}{MR}; \quad \Lambda_u = \frac{-I_\omega}{MR}$$

As stated previously, c_u is the control law and $m(u,\dot{u})$ is a function of uncertainties on u and $\dot{u}$ in the equations of the system dynamics. We have the following relationship:

$$\dot{u} = c_u - m(u,\dot{u}) \tag{18}$$

with the control law defined as:

$$c_u = \dot{u}_d + K_p^u \varepsilon_u + \sigma_u \tag{19}$$

and:

- $\dot{u}_d$, an anticipative term;
- $\varepsilon_u = u_d - u$, the velocity error;
- K_p^u, a positive constant that permits to define the settling time of the closed-loop system;
- σ_u, the sliding-mode control law.

Using the Lyapunov candidate function $V = \left(1/2\right)\varepsilon_u^2$, it can be immediately verified that the stability of the system is guaranteed by the choice of the sliding-mode control law$\sigma_u = \rho\frac{\varepsilon_u}{|\varepsilon_u|}$, with ρ a positive scalar, large enough to compensate the uncertainties on the longitudinal dynamics of the system.

2.4 Expression of the Global Control Law

In practice, uncertainty about the dynamics of the system to control leads to uncertainty in the sliding hyperplane $s = 0$. As a consequence $s \neq 0$ and the sliding control law s, which has a behavior similar to the signum function, induces oscillations while trying to reach the sliding surface $s = 0$ with a theoretically zero time. These high-frequency oscillations around the sliding surface, called chattering, increase the energy consumption and can damage the actuators. In order to reduce them, we can replace the signum function by an arctan function or, as chosen here, by adding a parameter with a small value ν in the denominator. So, we use the function $\frac{s}{|s|+\nu}$.

Finally, the following torques are applied to each of the N wheels:

$$\tau_i = \frac{1}{N}\left(\tau_u - \frac{R}{w_i}\tau_\theta\right) \tag{20}$$

with τ_u and τ_θ re-computed with a change of variable, from the inverse of the robot dynamics model—equations (17) and (4) with the accelerations $\dot{u}$ and $\dot{\theta}$ replaced respectively by the control laws (19) and (14)—namely,

$$\tau_u = \frac{1}{\gamma}\left(\dot{u}_d + K_p^u\varepsilon_u + \rho\frac{\varepsilon_u}{|\varepsilon_u| + \nu_u} - \Lambda_u\sum_{i=1}^{N}\dot{\omega}_i - rv\right) \tag{21}$$

$$\tau_\theta = \frac{1}{\lambda}\left(\dot{\tilde{r}}_d + K_p^\theta\varepsilon_\theta + K_d^\theta\dot{\varepsilon}_\theta + \mu\frac{\mathbf{B}^T\mathbf{P}\mathbf{x}}{|\mathbf{B}^T\mathbf{P}\mathbf{x}| + \nu_\theta} - \Lambda_\theta\dot{\omega} - \mathbf{D}_\theta\mathbf{F}_y\right) \tag{22}$$

To estimate the value of the lateral forces $\mathbf{F}_y$, Pacejka theory [11] could be used, by taking into account the slip angle. Because of the robustness of the sliding-mode control, however we can consider that $\mathbf{F}_y$ is a perturbation to be rejected, and we do not include it in the control law. A slip-angle measure being in practice not very efficient, this solution is better.

3 Application to the RobuFAST A Robot

3.1 Experiments

3.1.1 Control Law Implementation

The sliding-mode control law is tested with the RobuFAST A robot on a slippery flat ground. This experimental platform, shown in Fig.3, consists of an electric off-road vehicle, whose maximum reachable speed is 8 m/s. Designed for all-terrain mobility, the robot can climb slopes of up to 45° and has the properties displayed in Table 1. The front and rear directions of the vehicle are blocked to allow the skid-steering mode operation.

Total mass	$M = 350\ kg$
Yaw inertia	$I_z = 270\ kg.m^2$
Wheelbase	$l = 1.2\ m$
Rear half-wheelbase	$w = 0.58\ m$

Table 1 Experimental robot inertial parameters

The implementation of the control law in real-life conditions requires some measures and observations. In particular the norm of the velocity vector, measured by the GPS, must be decomposed into its lateral and longitudinal components. This decomposition is made possible by the addition of an observer of the slippage angle [12], the knowledge of this angle and the velocity vector norm allowing us to make a projection on the axes of the robot frame.

The controller is implemented in two steps: first, a proportional derivative controller is settled for path following; then, the sliding-mode controller is added and its gains tuned.

This sliding-mode controller being a torque controller, a difficulty is that the robuFast A robot inputs are its wheel velocities. It is thus necessary to convert the amplitude of the torques generated by the controller.

Referring to eq.(3) of the wheel dynamics, we can consider that the addition of a force differential in a wheel is equivalent to a differential in its angular acceleration, i.e.,

$$\Delta\dot{\omega} \equiv \frac{R}{I_\omega}\Delta F$$

The losses in the movement transmission, due to wheel-soil contact, are disturbances to be compensated by the robust controller. This method is justified in particular in a patent [13].

The value of I_ω is obtained by the sum $I_\omega = I_{eq} + I'_\omega$. For a Marvilor BL 72 motor of a mass of $2.06kg$ and a reduction gear with $K = 16$, we have $I_\omega = 0.364kg.m^2$,

where I'_ω is the wheel inertia and $I_{eq} = K^2 I_m$ is the inertia equivalent to the motor and reduction gear unit, with K the reduction gear speed reducing ratio and I_m the motor inertia.

3.1.2 Experiment Results

The robot moves at a velocity of 3 m/s along a sinusoidal road. A derivative-proportional controller is applied to the robot, then the sliding-mode controller is implemented.

The position is plotted on figure 4 in m, the gains being tuned for optimum path-following: $K_p^u = 0.05\ s^{-1}$, $K_d^\theta = 0.02\ s^{-1}$, $K_p^\theta = {K_d^\theta}^2/4\zeta^2$, $\zeta = 0.70$, $T_r = 0.5\ s$, $\nu_u = 0.01\ ms^{-1}$, $\nu_\theta = 0.02$, $a = 0.10$, $b = 0.1$, $\mu = 0.1$ and $\rho = 0.01\ ms^{-2}$.

Fig. 3 RobuFAST A on site with its DGPS fixed base (upper left hand side)

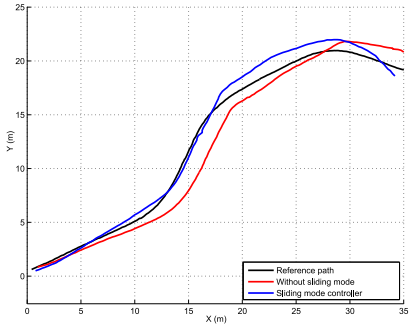

Fig. 4 Position (m)

Fig. 5, which indicates the curvature of the reference path as a function of the time, yields the robot position for the analysis of the evolution of its state variables in the time, the lateral error of Fig. 6, the yaw error of Fig. 7, the longitudinal velocity error of Fig. 8, and the torque inputs of Fig. 9 and Fig. 10.

Without sliding-mode, we see on the position curve that the vehicle follows the desired path with a small position offset. After a bend, the robot takes time to converge to the path. The succession of bends maintains this position error. With sliding-mode, the position curve converges much better to the desired path with however a small lateral error of about the length of a vehicle track, between the second and the third bend.

The delay of the actuators is due to the inertia of the vehicle slipping on a wet ground. There is almost no yaw-angle error during this period, as we can see at around a time of 14 s on the sliding mode controller curve Fig. 7. There is thus only a lateral error to be corrected, which explains a slower convergence. The convergence time can be tuned with parameter d_0 of eq.(5), but too high a value will bring

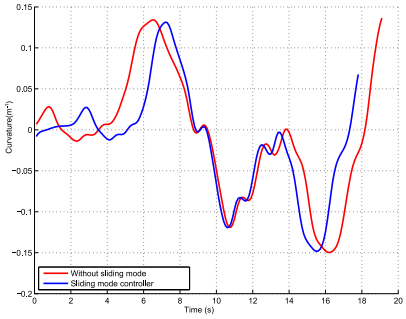

Fig. 5 Curvature of the path to follow during the time (1/m)

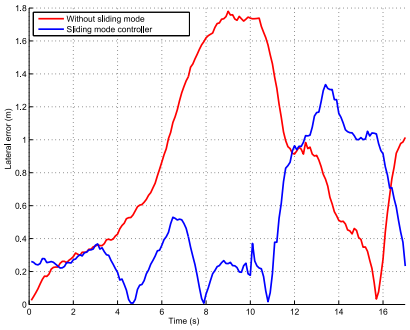

Fig. 6 Lateral error (m)

about the risk of yaw instability, which could occur during bend.
On the lateral error curves displayed on Fig. 6, we notice a good following until the

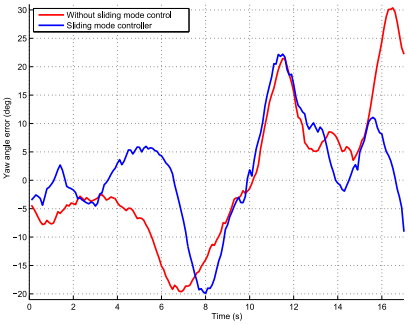

Fig. 7 Yaw angle error (deg)

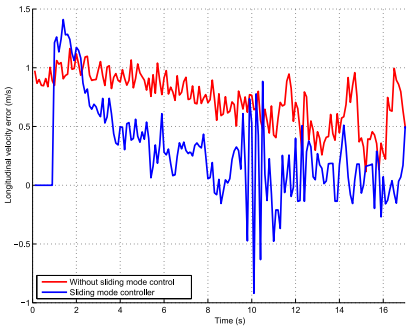

Fig. 8 Longitudinal velocity error (m/s)

second bend (11 s) with an error that remains under 0.6 m oscillating around 0.2 m, whereas the error reaches 1.8 m without sliding-mode.

There is no significant difference between the yaw error with and without the sliding-mode control law; however, after the last bend (15 s) the robot has some difficulties to reach the path without the sliding-mode controller. The longitudinal velocity error is globally well reduced with the sliding-mode controller, as we can see in Fig. 8. We observe the chattering phenomenon during the second bend (11 s), with the strong oscillations of the velocity curve.

To correct the velocity errors, higher torque values are applied with the sliding-mode controller (torque curve for the velocity regulation of the Fig. 10), stabilized around 30 Nm. On the torque curve for the yaw regulation, we observe few peaks for three bends (7 s, 11 s et 15 s), with higher values without sliding-mode because

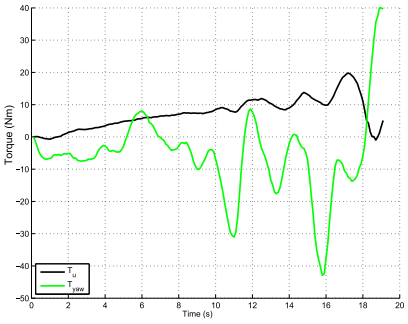

Fig. 9 Torques without the sliding-mode controller (Nm)

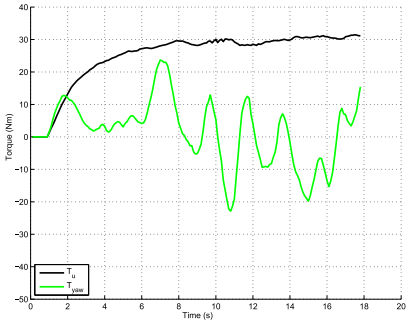

Fig. 10 Torques with the sliding-mode controller (Nm)

of larger errors to correct in order to reach the path.

Finally, during several trial days, we noticed an increase of the energy consumption of 20 % to 30 % with the sliding-mode controller, the robot batteries emptying faster because of a higher frequency request of the actuators. This last point is a constraint, the supply of energy being an important problem in mobile robotics. This control law could be used at intervals, when it turns out to be necessary.

4 Conclusions

The sliding-mode controller introduced here was tested in real-life conditions with a torque-controlled four-wheel skid-steering robot. It was proven to be robust on sinusoidal paths, and despite wheel slippage. The chattering noticed during the experiments led to a higher energy consumption. In order to reduce it, we defined the gain variables according to some criteria such as the velocity or the path curvature. If the energy consumption becomes a concern, a higher-order sliding-mode control law should be considered.

References

1. L. Caracciolo, A. De Luca, and S. Iannitti. Trajectory tracking control of a four-wheel differentially driven mobile robot. In *Proceedings of the IEEE International Conference on Robotics & Automation*, pages 2632–2638, Detroit, Michigan, May 1999.
2. K. Kozlowski and D. Pazderski. Modeling and control of a 4-wheel skid-steering mobile robot. *International journal of applied mathematics and computer science*, 14:477–496, 2004.
3. W.E. Dixon, D.M. Dawson, E. Zergeroglu, and A. Behal. *Nonlinear Control of Wheeled Mobile Robots*. London, 2001.
4. A. Jorge, B. Chacal, and H. Sira-Ramirez. On the sliding mode control of wheeled mobile robots. In *Systems, Man, and Cybernetics, 1994. 'Humans, Information and Technology'., IEEE International Conference on*, volume 2, pages 1938–1943, Oct 1994.
5. L. E. Aguilar, T. Hamel, and P. Souères. Robust path following control for wheeled robots via sliding mode techniques. In *IROS*, 1997.
6. J.-M. Yang and J.-H. Kim. Sliding mode control for trajectory tracking of nonholonomic wheeled mobile robots. In *IEEE*, 1999.
7. M.L. Corradini and G. Orlando. Control of mobile robots with uncertainties in the dynamical model: a discrete time sliding mode approach with experimental results. In Elsevier Science Ltd., editor, *Control Engineering Practice*, volume 10, pages 23–34. Pergamon, 2002.
8. F. Hamerlain, K. Achour, T. Floquet, and W. Perruquetti. Higher order sliding mode control of wheeled mobile robots in the presence of sliding effects. In *Decision and Control, and 2005 European Control Conference. CDC-ECC '05. 44th IEEE Conference on*, pages 1959–1963, 12-15 Dec. 2005.
9. D. Lhomme-Desages, Ch. Grand, and J.C. Guinot. Trajectory control of a four-wheel skid-steering vehicle over soft terrain using a physical interaction model. In *Proceedings of ICRA'07 : IEEE/Int. Conf. on Robotics and Automation*, pages 1164 – 1169, Roma, Italy, April 2007.
10. S. S. Sastry. *Nonlinear systems: Analysis, Stability and Control*. Springer Verlag, 1999.
11. H. B. Pacejka. *Tyre and vehicle dynamics*. 2002.
12. C. Cariou, R. Lenain, B. Thuilot, and M. Berducat. Automatic guidance of a four-wheel-steering mobile robot for accurate field operations. *J. Field Robot.*, 26:504–518, 2009.
13. T. Yoshikawa. Open-loop torque control on joint position controlled robots, October 2008.